

Complexation of a polyelectrolyte with oppositely charged spherical macroions: Giant inversion of charge.

T. T. Nguyen and B. I. Shklovskii

Department of Physics, University of Minnesota, 116 Church St. Southeast, Minneapolis, Minnesota 55455

Complexation of a long flexible polyelectrolyte (PE) molecule with oppositely charged spherical particles such as colloids, micelles, or globular proteins in a salty water solution is studied. PE binds spheres winding around them, while spheres repel each other and form almost periodic necklace. If the total charge of PE is larger than total charge of spheres, repulsive correlations of PE turns on a sphere lead to inversion of the net charge of each sphere. In the opposite case, we predict another correlation effect: under-screened by PE spheres bind to PE in such a great number that they invert charge of PE. The inverted charge by absolute value can be larger than the bare charge of PE even when screening by monovalent salt is weak. At larger concentrations of monovalent salt, the inverted charge can reach giant proportions. Our theory is in qualitative agreement with recent experiments on micelles-PE systems¹.

PACS numbers: 87.14Gg, 87.16.Dg, 87.15.Tt

I. INTRODUCTION

Electrostatic interactions play an important role in aqueous solutions of biological and synthetic polyelectrolytes (PE). One generic electrostatic problem of the polymer physics is the problem of complexation of a long flexible polyelectrolyte with oppositely charged spherical particles such as micelles¹, globular proteins² or colloids³. A long PE binds oppositely charged spheres winding around each of them (Fig. 1). Without losing the generality, we assume that PE is negative and spheres are positive.

If the charge of a sphere is not completely compensated by the winding PE, the net charge of the sphere is still positive, the neighbouring spheres repel each other and form on PE an almost periodic necklace. The same picture is true when winding PE inverts the net charge of each sphere making it negative. We call this nontrivial phenomenon a sphere charge inversion (SCI). SCI is known to happen in the most famous biological example of PE-spheres complexation. In the chromatin, a negative double-helix DNA molecule winds around a positive histone octamer to form a complex known as the nucleosome core particle. They are connected by DNA linkers in the so-called beads-on-a-string structure. When linkers are cut enzymatically each nucleosome core particle is found to have a negative net charge.

The counter-intuitive phenomenon of SCI attracted a lot of attention of theorists. However, all theoretical and numerical studies of SCI, have been done for the complexation a single sphere with PE.⁴⁻¹⁰

In this paper, we propose the first theory of SCI in the necklace-like complex of PE with many spheres. Our theory accounts for the interaction between different spheres. We argue that in this case, as in the case of a single sphere, SCI happens due to repulsive correlations of different turns of PE on the surface of spheres.

For many spheres, however, not only the net charge of

a sphere should be found, but simultaneously the number of spheres attached to PE is to be calculated. Therefore, the second and even more challenging problem is to determine the sign of the whole complex of PE with many spheres. Is it positive or negative at a given concentrations of PE, n_p , and spheres, n_s , in solution?

The standard Debye-Hückel and Poisson-Boltzmann theories of screening of PE by monovalent counterions leave the net charge of PE always negative. These theories, however, do not work for screening by strongly charged spheres which, as we mentioned above, form a correlated sequence, reminding a necklace or an one-dimensional Wigner crystal. One can call it a Wigner liquid, because the long range order in many practical situations is destroyed.

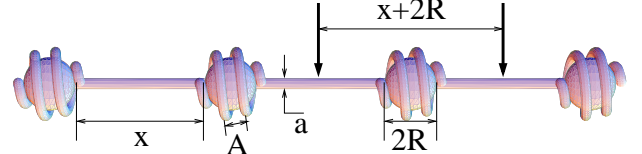


FIG. 1. The beads-on-a-string complex of a negative PE molecule and many positive spheres. On the surface of each sphere, due to Coulomb repulsion, neighbouring PE turns lie parallel to each other. Locally, they resemble a one-dimensional Wigner crystal with the lattice constant A . At larger scale, charged spheres repel each other and form one-dimensional Wigner crystal along the PE with lattice constant $x + 2R$. One Wigner-Seitz cell of this crystal is shown by the thick arrows.

Correlations, lead to an additional attraction of each sphere to PE. We show below that at large n_s and small n_p this leads to PE charge inversion (PECI). PECI was observed in a micelle-PE system¹.

Following Ref. 11-13 for a quantitative characteristic of charge inversion we introduce the charge inversion ratio of PE $\mathcal{P} = -Q^*/Q$, where Q is the negative bare

charge of PE and Q^* is its positive net charge together with absorbed spheres. Optimization of the free energy of a complex with respect of the number of bound spheres per PE molecule, N , shows that even for a large Debye-Hückel screening radius r_D of the solution the optimal $N = N_0$ is so large that

$$\mathcal{P} = \left(\frac{q}{R\eta\alpha} \right)^{1/4} \gg 1. \quad (1)$$

Here R and q is the radius and charge of a sphere and η is the linear charge density of PE, α is a dimensionless logarithmic function of $qR/\eta r_D^2$ (see Sec. III, case A.) We assume everywhere in this paper that $q/\eta R \gg 1$ so that more than one turn of PE winds around the sphere to neutralize it.

PECI also grows with stronger screening (smaller r_D). For r_D in the range $A \ll r_D \ll R(q/R\eta)^{1/2}$, we show that

$$\mathcal{P} = \sqrt{\frac{q}{r_D\eta\beta}} \gg \left(\frac{q}{R\eta} \right)^{1/4} \gg 1. \quad (2)$$

Here β is a dimensionless function of $q/R\eta$ and R/r_D (see Sec. V). A PECI given by Eq. (1) and Eq. (2) can be called giant.

At a large sphere concentration n_s , when the PE concentration, n_p , grows and reaches n_s/N_0 , the pool of free spheres gets exhausted and each PE can not get the optimal number N_0 any more. Then PECI becomes weaker and disappears linearly at the isoelectric point $n_{pi} = qn_s/|Q|$, where the total charge of all spheres compensates the total charge of all PE molecules. When the concentration n_p continues to grow beyond n_{pi} practically all spheres remain bound to PE and the net charge Q^* is negative and grows by absolute value. Variation of Q^*/Q with n_p is shown on Fig. 2 by solid line.

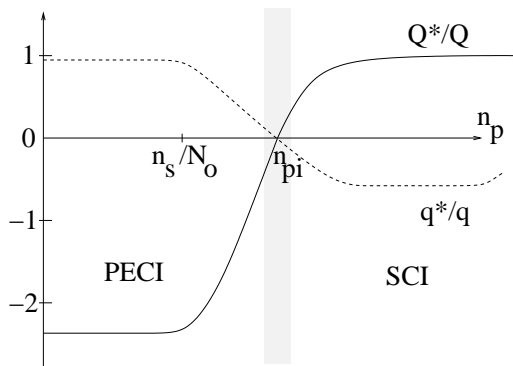


FIG. 2. Schematic plot of q^*/q and Q^*/Q as functions of the PE concentration, n_p , at a fixed and large sphere concentration n_s . Typical situation for not very large r_D is plotted. The shaded stripe corresponds to the condensation region around the isoelectric point $n_p = n_{pi}$.

Simultaneously with these variations of Q^*/Q , the net charge q^* of a sphere changes, too. At $n_p < n_s/N_0$ it is

positive and close to q . At $n_p > n_s/N_0$ the net charge q^* starts to decrease linearly with $n_p - n_{pi}$. At the $n_p = n_{pi}$ the charge q^* crosses zero and simultaneously, the linker length x vanishes. At $n_p > n_{pi}$, q^* becomes negative and SCI appears. We show that the charge inversion ratio of a sphere, $\mathcal{S} = -q^*/q$, grows with $n_p - n_{pi}$ until it reaches the value corresponding to a single sphere bound to infinite PE¹⁰, which is roughly equal to the inverse number of turns necessary for PE to neutralize a sphere. Behavior of q^*/q as function of n_p is shown by dashed line in Fig. 2. It is clear from Fig. 2 that SCI happens at $n_p > n_{pi}$ and PECI at $n_p < n_{pi}$.

Thus, we arrive at the conclusion that at $n_p > n_{pi}$ a beads-on-a-string structure can spontaneously self-assemble from a PE and oppositely charged spheres without any non-Coulomb forces.

Experimental observation of SCI is possible when spheres with winding PE are cut out from the complex. Then their charge can be measured by electrophoresis.

Consequences of PECI are more pronounced. Indeed, near the neutral point $n_p = n_{pi}$ each complex is almost neutral and short range attractive forces between Wigner-crystal-like complexes¹⁴ lead to their condensation and coarservation. Away from the neutral point each necklace complex is charged and the long range repulsive interaction prevents condensation. One can watch how condensation happens and disappears changing one of concentrations. For example, if we keep the spheres concentration n_s large and fixed and start from $n_p \gg n_{pi}$, the complexes are negative and repel each other. Then with decreasing n_p condensation happens in the vicinity of the isoelectric point (the shaded region in Fig. 2). If we continue decreasing n_p , PECI begins and the complexes become positive. When their positive charge, Q^* , becomes large enough the coarservate resolves. An important prediction of such theory¹⁵ is that the electrophoretic mobility changes sign in the coarservation range. We also able to estimate the width of the range of n_p around n_{pi} where coarservation occurs. This width increases with decreasing r_D and at $r_D \ll A$

$$\frac{\delta n_p}{n_{pi}} = \left(\frac{R\eta}{q} \right)^2 \frac{R}{r_D}. \quad (3)$$

The narrow range of coarservation followed by resolubilization was observed in a micelles-PE system¹ as a function of the charge of micelles. The electrophoretic mobility of complexes was indeed found to change sign within the interval of the micelle charge in which coarservation happens. The width of the coarservation region was also observed to increase with decreasing r_D in qualitative agreement with Eq. (3).

To illustrate the physical picture discussed above we carry out Monte-Carlo simulations of the complexation of a negative PE with two positively charged spheres. The system is in a salt free solution. The simulated spheres have charge $70e$ uniformly distributed over their surface and radius $3.5l_B$ where $l_B = 7.2\text{\AA}$ is the Bjerrum length

at the room temperature. The PE is modeled as a chain of free jointed hard spherical beads with radius $0.2l_B$ and charge $-e$. The bond length is kept fixed and equal to l_B . The Monte-Carlo algorithm is described in our previous paper (Ref. 10).

The snapshots of three such complexes are shown in Fig. 3. In the first simulation, the PE molecule has 70 monomers. This complex illustrates the regime where the spheres are in abundant ($n_p < n_s/N_0$). In the second simulation, the PE molecule has 140 monomers so that the complex is neutral and illustrates the condensation region around the isoelectric point $n_p = n_{pi}$. In the last simulation, the PE molecule has 210 monomers. This complex illustrates the regime where there are not enough spheres to neutralize the PE ($n_p > n_{pi}$).

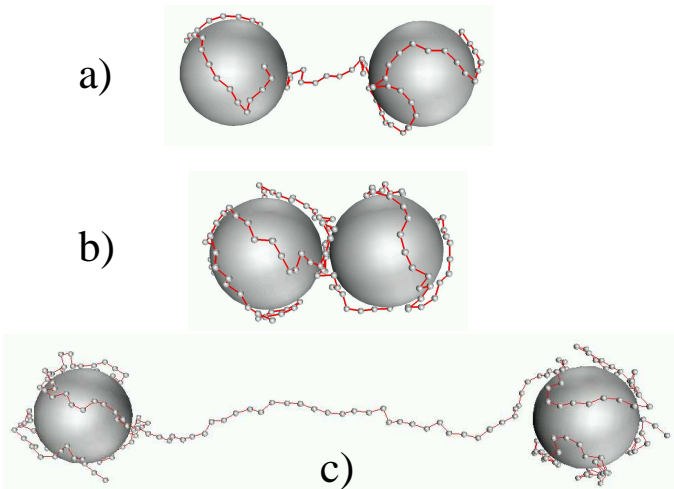


FIG. 3. Snapshots of three complexes of a negative PE with two positively charged spheres. The number of monomers in case (a), (b) and (c) are 70, 140 and 210 respectively. The spheres have charge $70e$. The total charges of the complexes are $70e$, 0 and $-70e$ correspondingly.

PECI is clearly observed in the first simulation. One PE with charge $-70e$ complexes with two spheres with charge $70e$ each making a giant 100% PEI. Around the isoelectric point, the distance between two spheres' surface is practically zero (less than the length of one PE bond l_B). Many such PE-spheres complexes condense into large bundles around the isoelectric point. Far beyond the isoelectric point, the PE-spheres complex is stretched again. SCI is observed with around 85 PE monomers bound to each sphere ($\sim 20\%$ SCI). Here, we also would like to mention recent Monte-Carlo simulations¹⁶ of complexation of a PE molecule with many oppositely charged spheres. Their results are in qualitative agreement with Fig. 2. However we cannot compare them with our theory quantitatively because in their simulations the parameter $q/R\eta$ is not large.

This paper is organized as following. In the next section, we study the free energy of the system and derive the equations for the equilibrium values of x and N . In

sections III and IV, these equations are solved for the weak screening case where the screening radius r_D is larger than the necklace period $x + 2R$. In Sec. V, we discuss condensation and resolubilization near the isoelectric point. Sec. VI is devoted to the strong screening case, $r_D \ll x + 2R$. We show that in this case PEI is much stronger. In Sec. VII, we derive the charge inversion ratio for a stiff (rod-like) PE and compare it to the result for a flexible PE obtained in previous sections. Finally, in the conclusion, we discuss important assumptions used in this work.

II. OPTIMIZATION OF THE COMPLEX STRUCTURE. WEAK SCREENING CASE ($r_D \gg x + 2R$).

Let us start by writing down the free energy of the complex of a PE with length L and charge density η winding around N oppositely charged spheres of charge q and radius R (see Fig. 1). First, we assume the complex is in a low salt solution so that the screening radius r_D is larger than the distance between two neighbouring spheres $x + 2R$. We call this situation the weak screening case. Taking into account that the length of the PE segment that winds around each sphere is $(L/N - x)$, we have

$$F(N, x) = \frac{Q^{*2}}{DN(x + 2R)} \ln N + Nf(x) \quad , \quad (4)$$

where

$$\begin{aligned} f(x) = & \frac{q^{*2}}{2RD} - \frac{2q^*\eta}{D} \ln \frac{x + 2R}{2R} + \\ & + (x + 2R) \frac{\eta^2}{D} \ln \frac{x + 2R}{2R} - (x + 4R) \frac{\eta^2}{D} \ln \frac{x + 4R}{4R} \\ & + (L/N - x) \frac{\eta^2}{D} \ln \frac{A}{a} + x \frac{\eta^2}{D} \ln \frac{x}{2a}. \end{aligned} \quad (5)$$

Here D is the dielectric constant of water. At a length scale greater than its period $x + 2R$, the complex is a uniform rod of length $N(x + 2R)$ and charge density $Q^*/N(x + 2R)$ and the first term in Eq. (4) is the self energy of this rod (the macroscopic self energy). The logarithmic divergence of this energy is cut off at small distances by $x + 2R$ and at large distances by the length

$$N(x + 2R) = \min \{r_D, N(x + 2R)\} \quad , \quad (6)$$

where $N(x + 2R)$ is the rod length. In the second term of Eq. (4), $f(x)$ accounts for the total energy of one period of the necklace. It is calculated as the energy of a Wigner-Seitz cell consisting of a sphere with two PE tails of length $x/2$. The first terms in Eq. (5) accounts for the self energy of the absorbed sphere with net charge q^* at the PE. The second term accounts for the interaction of the sphere with the tails, the third and fourth terms account for the interaction between the tails. The fifth and sixth terms are, respectively, the self energies of the PE

wound around the macroion (which is screened at distance A between turns) and of the two straight tails with length $x/2$. It should be noted that writing down the second of Eq. (4) as $Nf(x)$ we have neglected the difference between the end spheres with those in the middle of the PE. This is justified for a reasonably large value of N . It should also be noted that we neglected the entropy of the PE monomers in the tails and at the spheres surface. This is justified because the charge of the sphere is large and Coulomb energy is much larger than the thermal energy of PE.

As we will see later, when n_p is away from the isoelectric point n_{pi} , the tail length x is much larger than R . This helps to simplify Eqs. (4) and (5). Approximating $A \simeq R^2/(L/N - x)$ and keeping only terms of the highest order in the large parameter x/R , one can rewrite these equations as

$$F(N, x) = \frac{\delta^2}{x} N \ln \mathcal{N} + N f(x) \quad (7)$$

$$f(x) = \frac{(\delta + x)^2}{2R} - 2(\delta + x) \ln \frac{x}{R} - (L/N - x) \ln \frac{(L/N - x)a}{R^2} + x \ln \frac{x}{a} \quad , \quad (8)$$

where we introduce the PE length needed to neutralize one sphere $\mathcal{L} = q/\eta$ and

$$\delta = \mathcal{L} - L/N = Q^*/N\eta \quad , \quad (9)$$

so that $q^* = \eta(\delta + x)$. From now on, we also write the energy in units of η^2/D (hence, the energy has dimensionality of length).

At a given N , the optimum distance x can be calculated by minimizing the free energy $F(N, x)$ with respect to x . This gives, to the leading terms,

$$\frac{\partial F}{\partial x} = -\frac{\delta^2}{x^2} \ln \mathcal{N} + \frac{\delta + x}{R} - \ln \frac{x}{R} + \ln \frac{L/N - x}{R} = 0 \quad . \quad (10)$$

The physical meaning of each term in Eq. (10) is quite clear. When one brings a unit length of the PE from the sphere surface to their tails, thereby increasing x , the four terms of Eq. (10) are, respectively, the lowering in the system's macroscopic energy (with increasing x), the potential energy cost due to the attraction of the PE to the sphere, the potential energy gained due to the repulsion of two PE tails of each spheres and finally the cost in the correlation energy at the surface of the sphere. This last term - the correlation energy term - needs further clarification. If the PE turns wound around a sphere were randomly oriented, its self energy per unit length would be $\ln(R/a)$. In reality, due to strong lateral repulsion between different PE turns, they lie parallel to each other and locally resemble a one-dimension Wigner crystal. In this ordered state, the self energy per unit length of the PE turn is screened at distance A instead of R . This

gives the energy $\ln(A/a)$ per unit length of the PE. The lowering in the self energy of the PE in the ordered state as compared to the randomly oriented state is equal to $\ln(R/a) - \ln(A/a) = \ln(R/A) \simeq \ln((L/N - x)/R)$ and is called the correlation energy. The fourth term of Eq. (10) is its derivative with respect of x . A more detail discussion of this correlation effect can be found in Ref. 10.

In principle, one can (numerically) solve Eq. (10) for x as a function of N and other parameters of the system L/R and \mathcal{L}/R . After that, one can substitute $x(N)$ back into Eq. (7) and find the optimum value N_0 from the equation:

$$\left. \frac{dF(N, x(N))}{dN} \right|_{N=N_0} = \mu_s \quad , \quad (11)$$

where μ_s is the chemical potential of spheres in the solution.

If the PE concentration is small ($n_p < n_s/N_0$) then N_0 and $x(N_0)$ define the configuration of the complex. However, in the case $n_p > n_s/N_0$ there are less than N_0 spheres for each PE. In this case, $N = n_s/n_p$ (with an exponentially small correction) and $x(N)$ defines the configuration of the complex.

Let us now study asymptotic limits in which Eq. (10) can be solved analytically providing clear physical picture of our system.

III. A SINGLE POLYELECTROLYTE IN CONCENTRATED SOLUTION OF SPHERES. WEAK SCREENING CASE

In this section we consider the case where the PE concentration is small $n_p < n_s/N_0$ so that the optimization of $F(N, x(N))$ with respect to N is needed to get the optimum configuration of the complex. Here and everywhere in this paper we assume the sphere concentration is high enough so that one can approximate $\mu_s = \mathcal{L}^2/2R$ (the self energy of a bare sphere) neglecting the entropic part of the chemical potential. Eq. (11) can be rewritten as

$$\begin{aligned} \frac{\mathcal{L}^2}{2R} = \frac{dF}{dN} = \frac{\delta^2}{x} \left(1 + \frac{2L}{N\delta} - \frac{Nx'}{x} \right) \ln \mathcal{N} + \\ + \frac{(\delta + x)^2}{2R} \left(1 + \frac{2L}{N(\delta + x)} + \frac{2Nx'}{\delta + x} \right) - \\ - (2\mathcal{L} + x + Nx') \ln \frac{x}{2R} + (x + Nx') \ln \frac{L/N - x}{R} \end{aligned} \quad (12)$$

where $x' = dx/dN$.

To solve Eq. (10) for x , we assume that $\mathcal{L} \gg R \ln \mathcal{N}$ or, in other words, the screening length is smaller than an exponentially large length $r_D \ll x \exp(\mathcal{L}/R)$. As we will see later, in this case $\delta \gg x$ and the last two terms in Eq. (10) can be neglected. This gives

$$x = \delta^{1/2} (R \ln \mathcal{N})^{1/2} \quad . \quad (13)$$

Substituting Eq. (13) into Eq. (12) and keeping only the highest order terms one obtains the equation

$$(\delta R \ln \mathcal{N})^{1/2} (2\delta + 3L/N) - (L/N)^2/2 = 0, \quad (14)$$

which has consistent solution only if $\delta \gg L/N$. In this case,

$$\delta \sim \frac{L}{N} \left(\frac{L/N}{R \ln \mathcal{N}} \right)^{1/3}, \quad (15)$$

and the solution for $N_0 = L/(x + 2R)$ is

$$N_0 = \frac{L}{\delta^{3/4} (R \ln \mathcal{N})^{1/4}} \simeq \frac{L}{\mathcal{L}^{3/4} (R \ln \mathcal{N})^{1/4}}. \quad (16)$$

The corresponding charge inversion ratio is

$$\mathcal{P} = -\frac{Q^*}{Q} = \frac{N_0 \delta}{L} = \left(\frac{\mathcal{L}}{R \ln \mathcal{N}} \right)^{1/4} \gg 1. \quad (17)$$

From Eq. (13) and (15), it is easy to see that the relative order of all the length in the system is

$$\begin{aligned} \delta &\simeq \mathcal{L} \gg L/N = \mathcal{L}^{3/4} (R \ln \mathcal{N})^{1/4} \\ &\gg x = \mathcal{L}^{1/2} (R \ln \mathcal{N})^{1/2} \gg R \ln \mathcal{N} \gg R. \end{aligned} \quad (18)$$

This order is consistent with the assumptions we started with.

As we saw above, the two last logarithmic terms in Eq. (12) are negligible. Therefore, the main driving force behind PEI is the gain in the self-energy of the spheres when PE winds around it reducing its net charge. It is the difference between the left hand side and the second term of Eq. (12). In other words, the sum of the self-energies $q^{*2}/2RD$ decreases when PE distributes itself over large number of spheres. This correlation effect overcomes the macroscopic energy cost of overcharging the PE (the first term on the right hand side of Eq. (12)). Therefore, PEI can be well obtained in the approximation where PE charge is smeared on the surface of spheres^{5,6}.

Let us explain why we still call PEI calculated here a correlation effect. As we saw above the reason for this PEI is that each sphere is bound to several turns of a negatively charged PE. These turns can be considered as a correlation hole in the sense that this is the part of PE, which interacts almost exclusively with the given sphere (other spheres are at much larger distance $x \gg R$). The segments of PE wrapped around each sphere, $L/N - x \sim L/N \gg x$, have the same length. Therefore, similarly to Ref. 10–13 we are dealing with Wigner-crystal-like correlations and the wrapping segment can be considered as a Wigner-Seitz cell of the bare sphere (different from the one shown in Fig. 1). The gain in the sphere self-energy mentioned above is nothing but the usual chemical potential of a Wigner crystal: the interaction of a sphere with its Wigner-Seitz cell.

Note, however, that because most of the PE length is wrapped around the spheres, the periodicity of positions

of spheres covered by PE solenoids in the real space (see Fig. 1) is less important than in the case of a rigid PE (see Sec. VII) or other cases of charge inversion of rigid macroions by multivalent counterions^{11–13}. Linkers between different pairs of neighbouring spheres may differ in their length without a substantial change in the two major contributions to the free energy discussed above (the sphere self-energy gain and the macroscopic charging energy). The thermal motion can even melt the Wigner crystal of spheres in the real space while the length of the wrapping segment remains unchanged. Therefore charge inversion is much more robust than the Wigner crystal in real space.

IV. HIGH CONCENTRATION OF POLYELECTROLYTE. WEAK SCREENING CASE ($r_D \gg x + 2R$).

In this section, we deal with the case when $n_p > n_s/N_0$ and there are not enough spheres to supply each PE with the optimum number, N_0 , spheres found in previous section. In this case, the amount of spheres per PE is fixed: $N = n_s/n_p$. Therefore

$$\frac{Q^*}{Q} = \frac{Q - n_s q/n_p}{Q} = 1 - \frac{n_{pi}}{n_p} = \frac{\delta}{\mathcal{L}}, \quad (19)$$

so that PEI becomes weaker and linearly decreases with $n_p - n_{pi}$ as n_p grows. When n_p increases beyond the isoelectric point $n_{pi} = n_s q/Q$, the total charge of the complex Q^* is negative. The ratio Q^*/Q increases linearly from zero and eventually saturates at unity as n_p increases further. The behavior of Q^*/Q as function of n_p is plotted by the solid curve in Fig. 2.

Let us now discuss the behavior of the net charge of the sphere $q^* = \eta(\delta + x)$ as n_p increases. To do so, one has to solve Eq. (10) and find the distance x by which the spheres are separated along the PE (we stress again that we are interested in the complex far enough from the isoelectric point, so that $x \gg R$ and Eq. (10) is valid.)

As n_p increases beyond n_s/N_0 , the last two logarithmic terms in Eq. (10) are still negligible compare to the second term. Therefore, x is given by Eq. (13) (it should be noted that, here, $\delta = \mathcal{L}(1 - n_p/n_{pi})$ is a given length). Correspondingly, q^* decreases as δ .

As n_p moves closer to the neutral point, the net charge $q^* = \eta(\delta + x)$ decreases. When

$$\delta < \delta_c = R \ln \frac{L/N - x}{R} \simeq R \ln(\mathcal{L}/R), \quad (20)$$

(here, we replace $\ln((L/N - x)/R)$ by $\ln(\mathcal{L}/R)$ because near the isoelectric point, $\delta, x \ll \mathcal{L} \sim L/N$) the fourth and first terms of Eq. (10) start to dominate over the second and third terms. This gives

$$x \simeq |\delta| \sqrt{\frac{\ln \mathcal{N}}{\ln(\mathcal{L}/R)}}. \quad (21)$$

Of course, Eqs. (13) and (21) match each others at $\delta = \delta_c$. To continue, let us consider two important limiting cases $\ln \mathcal{N} \ll \ln(\mathcal{L}/R)$ and $\ln \mathcal{N} \gg \ln(\mathcal{L}/R)$.

A. The case $\ln \mathcal{N} \ll \ln(\mathcal{L}/R)$

In this case, $x \ll |\delta|$ and, therefore, the charge of a sphere $\eta(\delta + x)$, decreases to zero and becomes negative as n_p crosses n_{pi} (see Fig. 2). At $n_p > n_{pi}$, this SCI is driven by the fourth term of Eq. (10), the correlation energy of PE segment at the surface of the spheres. The charge inversion ratio $\mathcal{S} = |\delta + x|/\mathcal{L} \simeq |1 - n_p/n_{pi}|$ (see Fig. 2).

As n_p increases further, the charge of the sphere $\delta + x$ grows and the second and fourth terms of Eq. (10) becomes the dominant terms. This gives

$$q^*/\eta = \delta + x = -R \ln \frac{L/N - x}{R} \simeq -R \ln \frac{\mathcal{L}}{R}, \quad (22)$$

so that the charge inversion ratio reaches its maximal possible value (see Fig. 2) which is equal to that for the complexation of a single sphere and a polyelectrolyte¹⁰:

$$\mathcal{S} = \frac{-q^*}{q} \simeq \frac{R}{\mathcal{L}} \ln \frac{\mathcal{L}}{R}.$$

Therefore, roughly speaking, it is inversely proportional to the number of turns of PE around the sphere.

As n_p continues to increase, x increases and the third term of Eq. (10) becomes important making the sphere charge less negative. When $x > \mathcal{L}$, the second and third terms of Eq. (10) dominate. This gives

$$q^*/\eta = \delta + x = R \ln \frac{x}{R} \simeq R \ln \frac{L}{NR}, \quad (23)$$

so that the net charge of the sphere changes sign from negative back to positive (not shown in Fig. 2). However, the condition of low salt solution, $x < r_D$, assumed in the derivation of Eq. (10), makes this re-entrant inversion of charge unrealistic. In practical situation, $r_D < \mathcal{L}$ so that the necklace remains in the SCI range. A detail consideration of the strong screening case $r_D < x$ is presented in the next section.

B. The case $\ln \mathcal{N} \gg \ln(\mathcal{L}/R)$

In this case, Eq. (21) gives $x \gg |\delta|$ and the charge of a sphere $\eta(\delta + x)$ touches zero but stays positive as n_p crosses the isoelectric point despite the fact that the total charge of the complex $Q^* = N\delta$ changes from positive to negative. This is because for a long PE, the macroscopic energy is very large and the complex is under strong stress to increase x in order to reduce this macroscopic energy. This leads to a decrease in the amount of

PE that can wind around each sphere making the sphere positive.

As n_p increases beyond the isoelectric point, $|\delta|$, x and the net charge $q^* = \delta + x$ of each sphere increase as well. Eventually $q^* \simeq q$, the PE unwinds from all of its spheres and becomes a straight rod to which N spheres are attached to. Substituting $x = L/N$ into Eq. (10) and neglecting the last two terms of this equation, one can estimate the value L/N at which PE unwinds from the spheres: $L/N \simeq \mathcal{L}(1 + \sqrt{\mathcal{L}/R \ln \mathcal{N}})$. As n_p increases further, q^*/q saturates at unity. The behavior of q^*/q as the function of n_p is depicted by the dashed line in Fig. 3.

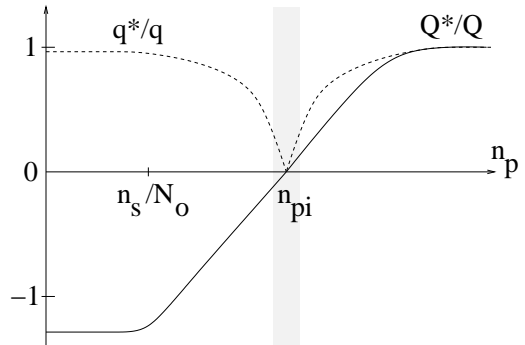


FIG. 4. Schematic plot of q^*/q and Q^*/Q as functions of PE concentration at a fixed and large sphere concentration n_s for the case B, Sec. IV. There is no SCI in this case. The shaded stripe shows the range of n_p around n_{pi} where condensation of PE molecules happens.

We would like to emphasize that the inequality $R \ln \mathcal{N} \gg \ln(\mathcal{L}/R)$ may require unreasonably large screening radius r_D , so that the behavior presented in Fig. 2 for case A of this section is more generic.

V. CONDENSATION OF PE-SPHERES COMPLEXES NEAR THE ISOELECTRIC POINT ($n_p = n_{pi}$).

Now, let us discuss the properties of the system near the isoelectric point. Exactly at the isoelectric point $n_p = n_{pi}$, the spheres-PE complex is neutral, $Q^* = q^* = \delta = x = 0$ and $L/N = \mathcal{L}$. From Eq. (7) one gets the energy of one complex as $L \ln(A/a)$. It is the self energy of the PE $L \ln(R/a)$ (the PE is straight up to distance R) plus the correlation energy $-L \ln(R/A)$ gained by arranging PE turns into one-dimensional Wigner crystal at the sphere surface (see the discussion after Eq. (10)). A consequence of this interpretation for the energy is that at the isoelectric point PE molecules condense onto each other forming a macroscopic neutral bundle. This is because the density of PE in the region where the spheres touch each other (the region bounded by broken line in Fig. 4) is doubled so the distance between PE segments is halved $A_t = A/2$ which results in a gain in the corre-

lation energy. Simple geometrical calculation shows that this region has the area AR . Therefore, the PE in this region has total length R . The correlation energy gain per unit volume is

$$\Delta E_{corr} \sim -\frac{n_p L}{\mathcal{L}} R \ln \frac{A}{A_t} \sim -\frac{n_p L}{\mathcal{L}} R .$$

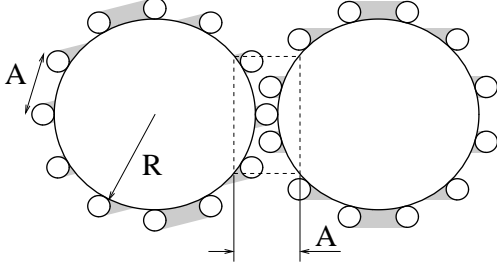


FIG. 5. Cross section through the centers of two touching spheres with worm-like (gray) PE wound around them. At the place where two spheres touch each others (the region bounded by the broken line) the density of PE doubles which in turn leads to a gain in the correlation energy of PE segments wound around the spheres. Near the isoelectric point, this gain is responsible for the condensation of spheres-PE complexes, forming a large neutral bundle of PE-spheres complexes.

Because of this finite gain in the correlation energy, there is a finite range of n_p around n_{pi} that the PE molecules are still in condensed state. Let us try to find the width of this region.

To find the boundary of the condensation region, on the left side of the isoelectric point ($n_p < n_{pi}$), one needs to compare the total energy of the system in the condensed state and dissolved state. Here, the condensed state contains a macroscopic neutral bundle of PE-spheres complexes and $(n_s - n_p L/\mathcal{L})$ leftover spheres per unit volume. The bundle is neutral because charging a macroscopic body costs a lot of energy. The dissolved state is a solution of n_p isolated PE-spheres complexes per unit volume, each PE absorbing n_s/n_p spheres. At the condensation concentration $n_p = n_{pl}$, we have to balance the correlation energy gain ΔE_{corr} with the lost in the self energy of $(n_s - n_p L/\mathcal{L})$ left-over spheres when they change from almost-neutralized spheres at the PE molecules to bare spheres in solution. Therefore the equation for the condensation point $n_p = n_{pl}$ is

$$\frac{n_p L}{\mathcal{L}} R = \left(n_s - \frac{n_{pl} L}{\mathcal{L}} \right) \frac{\mathcal{L}^2}{2R} \quad (24)$$

or

$$1 - \frac{n_p}{n_{pi}} \simeq \frac{R^2}{\mathcal{L}^2} . \quad (25)$$

On the right side of the isoelectric point ($n_p > n_{pi}$), the condensed state is a macroscopic neutral bundle of PE

and spheres and $(n_p - n_{pi})$ leftover bare PE molecules. ΔE_{corr} needs to be balanced with the lost in the self energy of PE molecules when they change from almost-neutralized state to bare state in solution. This gives for the resolubilization critical point n_{pr} :

$$\frac{n_{pi} L}{\mathcal{L}} R = (n_{pr} - n_{pi}) L \ln \frac{r_D}{a} \quad (26)$$

or

$$\frac{n_{pr}}{n_{pi}} - 1 \simeq \frac{R}{\mathcal{L} \ln(r_D/a)} . \quad (27)$$

Finally, the total width of the region, $\Delta n_p = n_{pr} - n_{pi}$, around n_{pi} where condensation occurs is

$$\frac{\Delta n_p}{n_{pi}} = \frac{R^2}{\mathcal{L}^2} + \frac{R}{\mathcal{L} \ln(r_D/a)} \simeq \frac{R}{\mathcal{L} \ln(r_D/a)} . \quad (28)$$

Comparing this with Eq. (20), we see that the width of the condensation region is small, well within the region where the correlation energy (the fourth term in Eq. (10)) is important in determining conformation of the system. Therefore, in this range ΔE_{corr} indeed dominates all other energies in Eq. (7) as we assumed.

VI. STRONG SCREENING BY MONOVALENT SALT ($r_D \ll x + 2R$).

Until now, we assumed the salt concentration is small enough so that the screening radius r_D is larger than the distance between neighbouring spheres, x . In the case of higher salt concentration when $r_D \ll x$, our theory needs some modifications. First, the macroscopic energy term (the first term in Eq. (4)) has to be replaced by the sum of the repulsion energies of neighbouring spheres. When $R \ll r_D \ll x$, it still has the form of interaction of two point-like charges:

$$F(N, x) = N \frac{q^{*2}}{x + 2R} e^{-(x+2R)/r_D} + N f(x) . \quad (29)$$

At the same time, all the logarithmic factors in Eq. (5) for $f(x)$ are cut off at r_D instead of x . Correspondingly, Eq. (10) (which is the result of the minimization of $F(N, x)$ with respect to x at a given N) should be replaced by

$$\begin{aligned} \frac{\partial F}{\partial x} = & -\frac{(\delta + x)^2}{x r_D} e^{-x/r_D} + \frac{\delta + x}{R} - \ln \frac{r_D}{R} \\ & + \ln \frac{L/N - x}{R} = 0 . \end{aligned} \quad (30)$$

Let us concentrate on the PECI regime when $n_p < n_s/N_0$. In this case, the last two logarithmic terms in Eq. (30) can be neglected. This gives

$$x = r_D \ln \frac{(\delta + x)R}{r_D x} \simeq r_D \ln \frac{\mathcal{L}R}{r_D^2} , \quad (31)$$

so that $r_D \ll x \ll \delta \sim \mathcal{L}$. One can see that x only weakly depends on the number N of spheres attached to the PE. This is because the macroscopic self-energy of the complex which forces the PE to unwind from the sphere is strongly screened and diminished.

Substituting Eq. (31) back into Eq. (29) and optimizing $F(N, x(N))$ with respect to N , we have, to the leading term

$$\frac{(L/N)^2}{2R} = \frac{r_D(\delta + x + 2L/N)}{R} + \frac{\mathcal{L}x}{R}, \quad (32)$$

so that

$$\frac{L}{N} = \sqrt{\mathcal{L}x} = \sqrt{\mathcal{L}r_D \ln \frac{\mathcal{L}R}{r_D^2}} \quad (33)$$

and the charge inversion ratio is

$$\mathcal{P} = \frac{N\delta}{L} = \sqrt{\frac{\mathcal{L}/r_D}{\ln(\mathcal{L}R/r_D^2)}}. \quad (34)$$

Comparing these results with those of Sec. III we see that due to screening, the spheres are closer to each other ($x \propto r_D$ instead of $\mathcal{L}^{1/2}R^{1/2}$) and smaller length of the PE is wound around a sphere. In other words, the positive net charge of each sphere is larger ($L/N \propto \mathcal{L}^{1/2}r_D^{1/2}$ instead of $\mathcal{L}^{3/4}R^{1/4}$). Therefore, more spheres are attached to the PE, making charge inversion much stronger ($\mathcal{P} \propto \mathcal{L}^{1/2}$ instead of $\mathcal{L}^{1/4}$). At the same time, when r_D increases to about $\sqrt{\mathcal{L}R}$, $x \sim r_D$, $L/N \simeq \mathcal{L}^{3/4}R^{1/4}$, $\mathcal{P} \simeq (\mathcal{L}/R)^{1/4}$ and we come back to the weak screening case.

It should be stressed that, for optimization with respect to x , the gain in a sphere's self energy when PE winds around the sphere (the second term on the right side of Eq. (30)) is balanced with the repulsion from its neighbouring spheres (the first term). However, when determining N and \mathcal{P} from Eq. (32), the repulsion between the spheres described by the first term on the right side, which is of the order $\mathcal{L}r_D/R$, is negligible compared to the second term $\mathcal{L}x/R$. This term originates from the fact that when one brings a sphere from solution to the PE, hence gains the self energy $(L/N)^2/2R$, the PE unwinds from other spheres in order to prepare the linker x for this new sphere.

Let us now consider even smaller screening radius $r_D \ll R$. In this case, one has to modify all the energy terms of Eq. (29). The self energy of each sphere becomes $q^{*2}r_D/2R^2$ instead of $q^{*2}/2R$ and the interaction between neighbouring spheres is

$$\frac{(q^*r_D^2/R^2)^2}{x} e^{-x/r_D}.$$

As a result, the minimization with respect to x gives

$$x = r_D \ln \frac{(\delta + x)r_D^2}{xR^2} \simeq r_D \ln \frac{\mathcal{L}r_D}{R^2}. \quad (35)$$

Now, an equation similar to Eq. (32) gives

$$\frac{L}{N} = \sqrt{\mathcal{L}x} = \sqrt{\mathcal{L}r_D \ln \frac{\mathcal{L}r_D}{R^2}} \quad (36)$$

and

$$\mathcal{P} = \frac{N\delta}{L} = \sqrt{\frac{\mathcal{L}/r_D}{\ln(\mathcal{L}r_D/R^2)}}, \quad (37)$$

so that the charge inversion is indeed stronger in this case and increases even faster than Eq. (34) with decreasing r_D . Eq. (34) and (37) match each other when $r_D \sim R$. Eq. (2) is their combination.

When the screening length becomes smaller than R^2/\mathcal{L} , the logarithmic factor $\ln(\mathcal{L}r_D/R^2)$ should be replaced by unity and Eqs. (35) and (36) give $L/N \sim R$ and $x \ll R$. This means that PE is a straight rod with the bare spheres closely packed on it. The number of spheres attached to the PE reaches its maximal possible value $N = N_{\max} = L/R$, and so does the charge inversion ratio $\mathcal{P} = \mathcal{P}_{\max} = \mathcal{L}/R$. The behavior of \mathcal{P} as a function of the screening length r_D is shown by the solid line in Fig. 6.

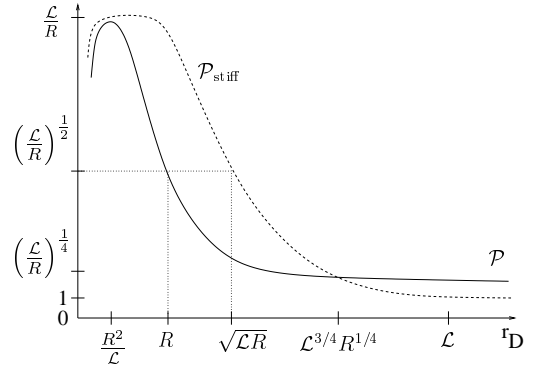


FIG. 6. Schematic plot of the charge inversion ratios \mathcal{P} (the solid line) and $\mathcal{P}_{\text{stiff}}$ (the dashed line) as function of screening length r_D . $\mathcal{P}_{\text{stiff}} > \mathcal{P}$ at $r_D \ll \mathcal{L}^{3/4}R^{1/4}$. \mathcal{P} saturates when $r_D \sim R^2/\mathcal{L}$ while $\mathcal{P}_{\text{stiff}}$ saturates when $r_D \sim R$. For the definition of $\mathcal{P}_{\text{stiff}}$, see Sec. VII.

It should be noted that at very small value of the screening length, when the energy of interaction between a sphere and the PE is less than $k_B T$, the spheres detach from the PE and \mathcal{P} rapidly decreases to zero.

Until now we have concentrated on the effect of strong screening on the optimal configuration of the PE-spheres complex at small concentration $n_p < n_s/N_0$, when spheres are in abundance. Now we want to discuss the role of screening in the opposite case, $n_p > n_s/N_0$. In this case, the number of spheres per PE $N = n_s/n_p$ is fixed and Eq. (19) remains valid (screening does not affect Q^* , because in any case all spheres are absorbed by PE.) Qualitatively, Fig. 2 remains valid in this case. The length x is now given by the first equality of Eq. (31) for

$r_D > R$ and by Eq. (35) for $r_D < R$ (the second equalities in these equations is not valid because δ is a given length). Therefore, x decreases as δ decreases.

In the case $r_D > R$, when δ decreases below r_D^2/R , Eq. (31) gives $x \leq r_D$ and we come back to the weak screening case described in Sec. IV, case A. All discussion about SCI and condensation of complexes in Sec. IV, case A remains valid in this case.

On the other hand, in the case $A < r_D < R$, our theory needs some correction. The value of δ below which the correlation energy between PE turns at the surface of a sphere is important is given by

$$\delta < \frac{R^2}{r_D} \ln \frac{L/N - x}{R} \simeq \frac{R^2}{r_D} \ln(\mathcal{L}/R) , \quad (38)$$

instead of Eq. (20). This is because, in this case, the second term in Eq. (10) is $(\delta+x)r_D/R^2$ instead of $(\delta+x)/R$.

At the same time, SCI effect at $n_p > n_{pi}$ is strongly enhanced in a way similar to the case of one sphere¹⁰. This is because the charging energy cost for SCI is strongly suppressed at small r_D while the short-range correlation energy between PE turns responsible for SCI remains unaffected. At small screening length, \mathcal{S} can be larger than unity.

Strong screening ($A \ll r_D \ll R$) also affects the range of n_p where PE molecules form neutral macroscopic bundle. When $r_D \ll R$, the self energy cost $\mathcal{L}^2/2R$ in the right hand side of Eq. (24) has to be replaced by $\mathcal{L}^2 r_D/R^2$ per sphere while the short-range correlation energy on the left hand side remains unaffected. This increases the width of this region to

$$\frac{\Delta n_p}{n_{pi}} \sim \frac{R^3}{\mathcal{L}^2 r_D} + \frac{R}{\mathcal{L} \ln(r_D/a)} . \quad (39)$$

This width continue to grow with decreasing r_D . When $r_D \sim R^2/\mathcal{L} \sim A$, $R^3/\mathcal{L}^2 r_D \sim R/\mathcal{L}$ and the width more than doubles. When $r_D < A$, one can neglect the second term of Eq. (39) and arrive at Eq. (3). This equation predicts a strong growth of $\Delta n_p/n_{pi}$ with decreasing r_D , in qualitative agreement with experimental results of Ref. 1. It should be noted again that, as one see from comparison with Eq. (38), this coarservation range is well within the region of δ where the correlation energy between PE turns is the dominant energy term.

Finally, when $n_p \gg n_{pi}$, there is very small number of spheres per PE such that the length of the PE linker between them is larger than the optimum x given by Eq. (31) and (35), the linker is no longer straight and each sphere with PE wound around it behaves independent from each other. SCI saturates at that given for the case of one sphere - one PE complexation¹⁰.

VII. POLYELECTROLYTE WITH EXTREMELY LARGE PERSISTENCE LENGTH

In this section we assume that the PE has an extremely large persistence length such that it cannot wind around

a sphere. In this case, the PE is a straight rod to which the spheres are attached to. We are interested in the PECI regime where the concentration of spheres is large.

For a rod-like PE, $x = L/N$, $Nx' = -L/N = -x$, $\delta + x = \mathcal{L}$. In the case of weak screening, $r_D \gg L/N$, Eq. (12) can be rewritten as

$$\mathcal{L} \frac{N\delta}{L} \ln \mathcal{N} \simeq \mathcal{L} \ln \frac{L/2N}{R} . \quad (40)$$

The physical meaning of this equation is very simple: the left hand side is the macroscopic charging energy cost when a sphere is brought from the bulk solution to the PE. The right hand side is the gain in the correlation energy of the Wigner crystal of spheres along the PE which helps to overcome the charging energy cost. This correlation energy is the interaction of the sphere with two PE tails of length $L/2N$ which forms a Wigner-Seitz cell.

The charge inversion ratio can be easily calculated

$$\mathcal{P}_{\text{stiff}} = \frac{N\delta}{L} = \frac{\ln(L/2NR)}{\ln \mathcal{N}} \simeq \frac{\ln(\mathcal{L}/R)}{\ln \mathcal{N}} . \quad (41)$$

In the case of strong screening, $r_D \ll L/N$, the macroscopic charging energy cost should be replaced by the repulsion between neighbouring spheres. At the same time, the logarithmic term in the expression for the correlation energy of the Wigner crystal of spheres along the PE should be cut off at r_D instead of L/N . Eq. (40) now reads:

$$\frac{\mathcal{L}^2}{r_D} e^{-L/Nr_D} = \mathcal{L} \ln \frac{r_D}{R} , \quad (42)$$

which gives $L/N \simeq r_D \ln(\mathcal{L}/r_D)$, and the charge inversion ratio

$$\mathcal{P}_{\text{stiff}} = \frac{N\delta}{L} \simeq \frac{\mathcal{L}}{r_D \ln(\mathcal{L}/r_D)} \gg 1 . \quad (43)$$

Let us now compare these results with those for a flexible PE case studied in Sec. III (weak screening) and Sec. V (strong screening).

At weak screening (Sec. III) $r_D > \mathcal{L} > R \ln \mathcal{N}$, Eq. (17) and Eq. (41) give

$$\frac{\mathcal{P}_{\text{stiff}}}{\mathcal{P}} = \frac{R \ln(\mathcal{L}/R)}{\mathcal{L}^{1/4} (R \ln \mathcal{N})^{3/4}} \simeq \frac{\ln(\mathcal{L}/R)}{(\mathcal{L}/R)^{1/4} (\ln \mathcal{N})^{3/4}} \ll 1 .$$

The last inequality is due to $\mathcal{L}/R \gg 1$ and $\ln \mathcal{N} \gg 1$.

As r_D decreases further so that $\mathcal{L} > r_D > \sqrt{\mathcal{L}R}$ we enter the strong screening regime for the rod-like PE but still stay in the weak screening regime for flexible PE. Using Eq. (43) for $\mathcal{P}_{\text{stiff}}$ and Eq. (17) for \mathcal{P} , we can easily see that the charge inversion for the rod-like PE starts to become stronger than charge inversion for the flexible PE when $r_D \sim \mathcal{L}^{3/4} R^{1/4}$.

When r_D continues to decrease in the range $r_D < \sqrt{\mathcal{L}R}$, we are in the strong screening regime for both

types of PE. Eq. (34) and (37) show that \mathcal{P} is of the order of $\sqrt{\mathcal{L}/r_D}$ which is much smaller than $\mathcal{P}_{\text{stiff}} \simeq \mathcal{L}/r_D$.

The behavior of the charge inversion ratio as a function of r_D for the two types of PE is shown in Fig. 6. One can explore a transition from the flexible PE case to the stiff PE case by applying an external stretching force to the PE¹⁷. To describe this phenomenon, one has to add to the free energy (7) of the complex an additional term $-\mathcal{F}N(x+2R)$, where \mathcal{F} is the external force. This new term is linearly proportional to the length of the spheres-PE complex. It adds a negative term $-\mathcal{F}$ to the right hand side of Eq. (10) and therefore increases x . One then can proceed in exactly the same way as in Sec. III to find the conformation of the complex. At weak screening when $r_D \gg \mathcal{L}^{3/4}R^{1/4}$ (Sec. III), it is not difficult to show that x increases linearly with the strength of the external force when this force is small. At the same time, N_0 decreases linearly with \mathcal{F} so that one by one, the spheres leave the PE as the force increases and PEI becomes weaker. When $\mathcal{F} \sim (\eta^2/D)(\mathcal{L}/R - \ln N)$ (so that the force helps to balance the attractive potential of the sphere with the macroscopic repulsive potential of the complex), one obtains $x \sim L/N$ and the PE unwinds completely from the spheres and becomes straight. The problem of complexation of PE and spheres, then, becomes that of a stiff PE described at the beginning of the section. This sequential release of spheres is similar to the problem of stretching a PE necklace in poor solvent¹⁸.

The picture is completely reversed at the strong screening case when $r_D \ll \mathcal{L}^{3/4}R^{1/4}$. In this case, as one stretches the PE, the spheres come to the PE one by one and make the charge inversion stronger. The strength of the force at which PE unwinds completely from the spheres can be calculated in exactly the same way as in the weak screening case. In the strong screening case, however, the macroscopic repulsive potential of the complex is very small so that the external force has to overcome only the attractive potential of the sphere in order to unwind the PE molecule. Therefore, PE unwinds completely when $\mathcal{F} \sim \eta^2\mathcal{L}/RD$ for $r_D > R$ and $\mathcal{F} \sim \eta^2\mathcal{L}r_D/R^2D$ for $r_D < R$.

It would be interesting to verify experimentally that the spheres leave the PE at weak screening and condense on the PE at strong screening when the PE undergoes an external stretching force.

VIII. CONCLUSION

In conclusion, we would like to discuss most important approximations used in this papers. Let us start from the use of the Debye-Hückel linear theory to describe screening by monovalent salt. It is known that if a PE molecule or a sphere are charged strongly enough this linear approximation does not work and nonlinear condensation of counterions takes place, which leads to a

renormalization of their charge. For the case of a rod-like PE this phenomenon is known as the Onsager-Manning condensation¹⁹. It happens when the linear charge density of PE η is larger than $\eta_c = Dk_BT/e$, where k_B is the Boltzmann constant and T is the temperature. Correspondingly, Debye-Hückel theory used above is valid when $\eta < \eta_c$.

The condition for the absence of counterion condensation on the charged spheres is more complicated and involves the concentration of monovalent salt as well. It is known that if a sphere is charged strongly enough, its counterions condense onto its surface to reduce its charge to the universal critical value $q_c = DRek_BT \ln(c_s/c)$, where e is the elementary charge, $c_s \sim q_c/R^3e$ and c are the counterion concentrations at the sphere surface and in the bulk respectively²⁰. The condensation on the spheres can be neglected if q is less than q_c or

$$r_D > Re^{\mathcal{L}\eta/R\eta_c} \quad . \quad (44)$$

At small enough η (such that $\eta/\eta_c < R/\mathcal{L}$), this condition reduces to $r_D > R$.

When $r_D < R$, each sphere can be considered as a plane with charge $q/4\pi R^2$ and it is also known that if r_D is small enough, a charged plane is linearly screened. Specifically, Eq. (73) of Ref. 13 shows that screening is linear if

$$r_D < Ae^{\eta_c/\eta} \sim \frac{R^2}{\mathcal{L}}e^{\eta_c/\eta}. \quad (45)$$

At small enough η (such that $\eta/\eta_c < R/\mathcal{L}$), this condition reduces to $r_D < R$.

Thus our theory has a wide range of applicability. For a PE with

$$\eta < \eta_c R/\mathcal{L} \quad (46)$$

it is applicable for any value of the screening length r_D . Remarkably, the same inequality for η also guarantees that no Onsager-Manning condensation occurs on the spheres-PE rod-like complex with the inverted charge $\eta\mathcal{P}$, even though the magnitude of this inverted charge can be much larger than the bare charge of the PE ($\mathcal{P} \gg 1$). Indeed, as we already know, \mathcal{L}/R is the maximal possible value for \mathcal{P} (see Fig. 5) therefore Eq. (46) guarantees that $\eta\mathcal{P}$ is smaller than the Onsager-Manning critical linear charge density η_c .

On the other hand, our theory literally is not applicable to strongly charged PE such as double helix DNA or too strongly charged spheres. We do, however, believe that our main results are qualitatively applicable in this case with properly normalized charges of the spheres and PE. A more detail study of condensation problem will be the subject of a future work.

Second approximation which we want to address here is the assumption that PE is flexible. It is valid if elastic energy of PE winding around a sphere is smaller than Coulomb energy of complexation. This can be true even if the persistence length of the strongly screened PE is

of the order of a sphere diameter or somewhat larger. For example, theoretical estimates show that even in the nucleosome, the rigidity of DNA plays a secondary role. If this persistence length is much larger than R , ground state of the complex can strongly differ from that in the flexible case. In Sec. VI we studied the extreme case when persistence length is infinite and the PE is rod-like. There is a wide range of intermediate magnitudes of persistence length which is not studied here. In this range nontrivial star-like configurations become possible even for one sphere²¹. For many spheres one can imagine different kind of structures. Near isoelectric point it can be a rod-like complex made of PE solenoid densely stuffed by spheres. It can be a similar cylinder where PE is instead winding around spheres makes several parallel to the cylinder axis straight strands on the surface of the cylinder, which are connected by loops at the cylinder edges. These strands repel each other and form periodic in polar angle "Wigner crystal". These and other possible configurations should be studied in future works.

The third simplification used in this paper was an assumption that the number and the size of spheres in the solution is fixed. When we try to compare this theory with the data on micelles-PE system¹ we immediately see that, strictly speaking, this is a different problem, because in experiment of Ref. 1 the amount of lipids is fixed, but a number and size of micelles is determined by equilibrium conditions and may depend, for example, on the screening radius of the solution. This complication should be taken into account by a future theory.

The fourth important assumption we made in this paper is that the concentration of spheres, in the solution, n_s , is large enough so that their entropy can be neglected. This assumption leads, for example, to the conclusion that in the case $n_p > n_s/N_0$, all the spheres are consumed by PE. Actually, even in this case, there is a finite, but exponentially small concentration of free spheres in the solution next to PE, n_{s0} , because the binding energy of a sphere to PE is finite. In other words, this is the concentration of the "saturated vapour" of spheres right above the correlated liquid of spheres on PE. When total concentration of spheres, n_s , is so small that it is comparable to n_{s0} effect of free spheres becomes very important. For example, at such small n_s spheres fail to neutralize PE near isoelectric point. At the limit of $n_p \rightarrow 0$ neutralization happens at $n_s = n_{s0}$. Therefore, the plot of the line $n_s(n_p)$ at which neutralization takes place deviates from isoelectric line $n_s = n_p L/\mathcal{L}$ at small n_p and n_s (see dashed line at Fig. 6). Correspondingly, range of the region of the condensation of PE-spheres complexes on the plane (n_s, n_p) looks as shown in Fig. 6 by shading.

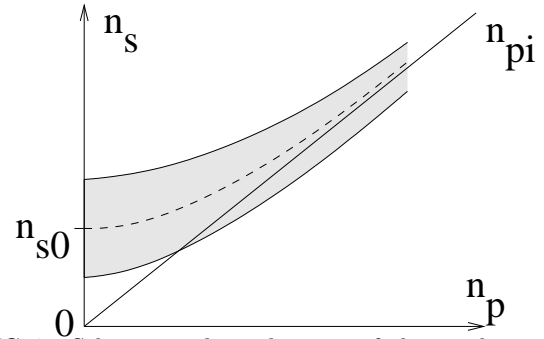


FIG. 7. Schematic phase diagram of the condensation of spheres-PE complexes in the (n_p, n_s) -plane for very large PE length L . Complexes condense in the shaded domain. Straight line correspond to the isoelectric point $n_s = n_p L/\mathcal{L}$. The dash line shows $n_s(n_p)$ at which an isolated PE-spheres complex is neutral.

Theory of condensation at small n_p is similar to theory of condensation of DNA by multivalent counterions at small concentration of DNA¹⁵. Experimental data on re-entrant condensation of DNA have qualitatively similar shape of the condensation domain²².

Summarizing our results, we have studied complexation of a negative PE with positive spherical macroions in salty water. Under solely the influence of electrostatic interactions, a PE molecule winding around individual spheres binds spheres in a beads-on-a-string structure. At large sphere concentration, we found interesting phenomena on both sides of isoelectric point, at which total charge of all PE molecules is exactly compensated by total charge of spheres. At concentration of PE below isoelectric point spheres overcharge PE so that the net charge of PE together with bound to it spheres is positive and can be substantially larger than the absolute value of the bare charge of PE. When concentration of PE exceeds the isoelectric point the net charge of PE is not inverted, while the net charge of each sphere together with PE winding around it becomes inverted and negative. It can be larger than the bare charge of the sphere if screening radius of the solution is small enough.

In the narrow vicinity of the isoelectric point PE-spheres complexes condense together in bundles. We calculated the width of the range of the PE concentration where the condensation takes place and showed that it grows very fast with decreasing screening radius of the solution.

All these phenomena are results of repulsive correlations between PE turns on the surface of spheres and of the spheres on PE, which can not be included in any Poisson-Boltzmann-like description of the mutual screening of PE and spheres. The repulsive correlations between PE turns on spheres are responsible for charge inversion of individual spheres (SCI) and the condensation of PE-spheres complexes in bundles. In the latter case this phenomenon is illustrated by Fig. 5. In the former case, additional discussion of the physics of this phenomenon can be found in Ref. Nguyen3. Wigner-

crystal-like correlations of turns mean that each turn is surrounded by a stripe of positively charge macroion surface, which can be considered as its positive correlation hole.

The most interesting phenomenon of the inversion of charge of PE (PECI) by large number of absorbed spheres is related to the fact that each sphere is bound to several turns of negatively charged PE. These turns can be considered as an correlation hole, because this is the part of PE, which almost exclusively interacts with the given sphere. In this sense, once more we are dealing with correlations. The segments of PE wrapping around each sphere have the same length and constitutes most of the PE's total length. Therefore, these correlations are similar to Wigner-crystal-like correlations which are responsible for charge inversion of a rigid macroion¹¹⁻¹³. This confirms our point of view that correlations are the universal driving force of charge inversion.

ACKNOWLEDGMENTS

We are grateful to A. Yu. Grosberg for helpful discussion and reading of the manuscript. This work was supported by NSF DMR-9985985.

-
- ¹ Y. Wang, K. Kimura, Q. Huang, P. L. Dubin, W. Jaeger, *Macromolecules*, **32** (21), 7128 (1999).
² V. A. Kabanov, V. P. Evdakov, M. I. Mustafaev, A. D. Antipina, *Molekulyarnaya Biologiya*, **11** 52 (1976); J. Xia and P. L. Dubin, In the book "Macromolecular complexes in Chemistry and Biology" Edited by P. L. Dubin et al., Springer-Verlag, Berlin, 1994.
³ E. Braun, Y. Eichen, U. Sivan and G. Ben-Yoseph, *Nature*, **391**, 775 (1998)
⁴ T. Wallin, P. Linse, *Langmuir* **12** 305 7128 (1996).

- ⁵ E. M. Mateescu, C. Jeppersen and P. Pincus, *Europhys. Lett.* **46**, 454 (1999);
⁶ S. Y. Park, R. F. Bruinsma, and W. M. Gelbart, *Europhys. Lett.* **46**, 493 (1999);
⁷ J. F. Joanny, *Europ. J. Phys. B* **9** 117 (1999). R. R. Netz, J. F. Joanny, *Macromolecules*, **32**, 9013 (1999); **32**, 9026 (1999).
⁸ P. Sens and E. Gurovitch, *Phys. Rev. Lett.* **82**, 339 (1999)
⁹ P. Chodanowski and S. Stoll, *Macromolecules*, **32** 2000
¹⁰ T. T. Nguyen and B. I. Shklovskii, *Physica A* **276** (2000).
¹¹ V. I. Perel and B. I. Shklovskii, *Physica A* **274**, 446 (1999), B. I. Shklovskii *Phys. Rev. E* **60**, 5802 (1999).
¹² T. T. Nguyen, A. Yu. Grosberg and B. I. Shklovskii *Phys. Rev. Lett.* **85**, 1568 (2000).
¹³ T. T. Nguyen, A. Yu. Grosberg and B. I. Shklovskii *J. Chem. Phys.* **113**, 1110 (2000).
¹⁴ I. Rouzina and V. A. Bloomfield, *J. Phys. Chem.* **100**, 9977, (1996); N. Gronbech-Jensen, R. J. Mashl, R. F. Bruinsma, and W. M. Gelbart, *Phys. Rev. Lett.* **78**, 2477 (1997); B. J. Ha and A. J. Liu, *Phys. Rev. Lett.* **79**, 1289 (1997); R. Podgornik and V. A. Parsegian, *Phys. Rev. Lett.* **80**, 1560 (1998); J. J. Arenzon, J. F. Stilck, and Y. Levin, *cond-mat/9806358*. B. I. Shklovskii, *Phys. Rev. Lett.* **82**, 3268 (1999).
¹⁵ T. T. Nguyen, I. Rouzina, B. I. Shklovskii, *J. Chem. Phys.* **112**, 2562 (2000).
¹⁶ M. Jonsson and Per Linse, *J. Chem. Phys.*, submitted (09/2000).
¹⁷ This idea was suggested to us by A. Yu. Grosberg.
¹⁸ T. A. Vilgis, A. Johnner and J. F. Joanny, *Eur. Phys. J. E.* **2**, 289 (2000). M. N. Tamashiro and H. Schiessel, *Macromolecules* **33** 5263 (2000).
¹⁹ G. S. Manning, *J. Chem. Phys.* **51**, 924 (1969).
²⁰ M. Gueron, G. Weisbuch, *Biopolymers*, **19**, 353 (1980); S. Alexander, P. M. Chaikin, P. Grant, G. J. Morales, P. Pincus, and D. Hone, *J. Chem. Phys.* **80**, 5776 (1984); S. A. Safran, P. A. Pincus, M. E. Cates, F. C. MacKintosh, *J. Phys. (France)* **51**, 503 (1990); L. Belloni, Doctoral thesis, University of Paris IV (1982); *Chem. Phys.* **99** 43 (1985).
²¹ H. Schiessel, J. Rudnick, R. Bruinsma and W. M. Gelbart, to be published.
²² E. Raspaud, I. Chaperon, A. Leforestier and F. Livolant, *Biophys. J.* **77** 1547 (1999)